Extended Abstracts of the 2021 International Conference on Solid State Devices and Materials, VIRTUAL conference, 2021, pp600-601

SSDM2021
Lead Halide Perovskite Scintillators

F. Maddalena*[1,2], A. Xie[1,2], M. E. Witkowski[3], M. Makowski[3], W. Drozdowski[3], S. V. Springham[4], P. Coquet[1,2,5], B. Mahler[6], C. Dujardin[6], M. D. Birowosuto*[1], C. Dang*[1,2]

[1]CNRS International - NTU - Thales Research Alliance (Singapore); [2]School of Electrical and Electronic Engineering, Nanyang Technological Univ. (Singapore); [3]Institute of Physics, Nicolaus Copernicus Univ. in Torun (Poland); [4]National Institute of Education (Singapore); [5]Institut d'Electronique de Microélectronique et de Nanotechnologie, Univ. de Lille (France); [6]Univ. Claude Bernard Lyon 1 (France)
*E-mail: francesco_maddalena@ntu.edu.sg, mbirowosuto@ntu.edu.sg, hcdang@ntu.edu.sg

Abstract
Here we report the emission properties of low-dimensional perovskite materials: quantum dots and two-dimensional perovskites under high energy excitation from X-, gamma-ray, alpha particle, and thermal neutron, aimed towards fast-timed imaging and particle detection applications.

1. Introduction

Scintillators are materials that down-convert high energy radiation, i.e. X-rays, gamma-rays and other ionizing radiation with keV or MeV energies, into photons in the ultraviolet-visible spectrum that can be detected by conventional photodetectors. This is schematically shown in Fig. 1a. Scintillators have many applications, such as medical diagnostics, industrial quality control, and scientific research. Recently, hybrid organic-inorganic perovskites and perovskite quantum dots (QDs) have shown remarkable properties as scintillators, such as high light yields, fast radioluminescence decay and low afterglow [1-3]. In addition, two-dimensional (2D) lead halide perovskites have also shown great potential for light-emission and scintillation applications [4, 5]. However, there are currently only limited studies and direct comparisons of the scintillation properties of low-dimensional perovskites, either 2D or quantum dots (QDs). Here we show the emission properties of lead-based perovskite QDs and two-dimensional (2D) perovskite crystals under excitation at high photon energies and particles, aimed at practical radiation detection applications, including thermal neutron detection.

2a. Perovskite quantum dots

Perovskite QDs have usually cubic structure, as shown in Fig. 1b. and have shown strong emission intensities under high energy radiations, much higher than the 3D-perovskite counterpart, particularly at room temperature. $CsPbBr_3$-QDs in particular have reached light yields of 25,000 photons/MeV [6]. Here we demonstrate the X-ray scintillation imaging application as well. To achieve thicker layers, and some degree of pixels, of $CsPbBr_3$-QDs, we used a silicon matrix with etched holes (100 mm deep and 50 mm in diameter). The template holes were filled with $CsPbBr_3$-QDs as shown in Fig. 1c. The pixilation of the scintillator, under exposure to X-ray with emission of green light, is shown in the inset of Fig. 1c. Using the $CsPbBr_3$-QDs-filled silicon template, we conducted preliminary imaging tests, using a thin platinum wire as text object. Despite the low power X-ray source (8.0 keV; 1 mA; 35 keV), we obtain a rather sharp image as shown in Fig. 1d.

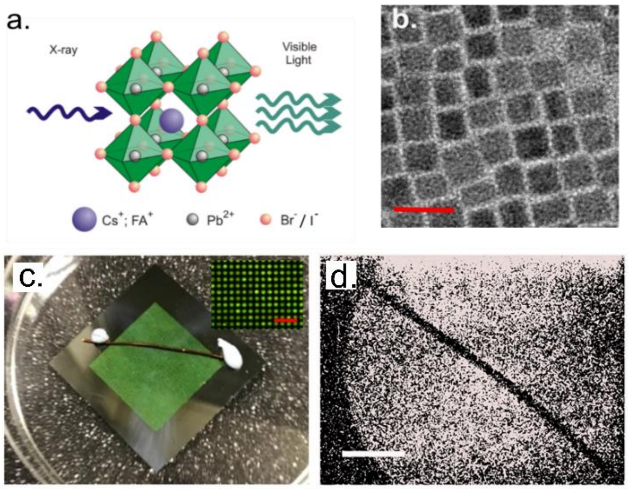

Fig. 1. a) Schematic depiction of a perovskite scintillator, where high energy X-rays are down converted into lower energy visible light. B) Transmission electron microscope image of $CsPbBr_3$-QDs. The scale bar is 20 nm. c) Bright-field image of a silicon substrates with capillary micro-holes filled with $CsPbBr_3$ quantum dots. Inset: Bright field image of a microcapillary plate filled with $CsPbBr_3$ quantum dots under UV excitation. b) X-ray imaging of a copper wire using the perovskite quantum dot filled silicon template shown in (c). A Cu-Ka source (8.0 keV; 1 mA; 35 keV) was used. Scale bar is 5 mm.

2b. Two-dimensional perovskites

2D-perovskite crystals, such as shown in Fig. 2a, also exhibit high light yield, in particular Lithium-doped phenylethyl-ammonium lead bromide (Li-PEA_2PbBr_4; 23,000 photons/MeV) [7] and butylammonium lead bromide (BA_2PbBr_4; 40,000 photons/MeV) [8]. The light yield was determined using the gamma-ray pulse height method, which results in quantitative values for the light yield and provides information on the energy resolution of the scintillator. In fact, the photo-peak to determine the light yield is especially observed strongly in single crystals since the radiation absorption is much more pronounced compared to polycrystalline films or quantum dots. The gamma-ray pulse measurement at different energies for BA_2PbBr_4 and Li-PEA_2PbBr_4 is shown in Fig. 2b. The normalized light yield and energy resolution for BA_2PbBr_4 and Li-PEA_2PbBr_4 are shown in Fig. 2c. Both materials show little variation in light yield with energy, good proportionality and show sharp energy resolutions around 10%, with Li-PEA_2PbBr_4 exhibiting the record of 7.7% at 662 keV.

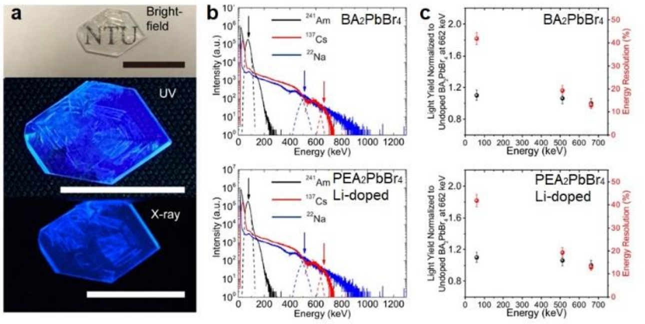

Fig. 2. a) PEA_2PbBr_4 single crystal under standard illumination (top), UV-light (middle) and X-ray excitation (bottom). b) Pulse height spectra under gamma-ray excitation with different sources for BA_2PbBr_4 (top) and Li-doped PEA_2PbBr_4 (bottom), with c) respective light yield and energy resolution values. The light yield was normalized to the value of undoped PEA_2PbBr_4 (11,400 ph/MeV).

Those 2D-structures also show potential for imaging. X-ray phase-contrast imaging of a steel safety pin was carried out using Li-PEA_2PbBr_4 thin film as scintillator, as schematically shown in Fig. 3a. The perovskite was spin-coated onto a glass substrate, forming a 67-μm thick film (Fig. 3b). The 2D-perovskite film shows high transparency and satisfying homogeneity, despite some small surface ripples. Despite the relatively small thickness of the scintillator, we obtained sharp pictures and the fine structure of the safety pin, like a 250-μm slit as shown in Fig. 2c. Here, the black and white mode was utilized for better contrast.

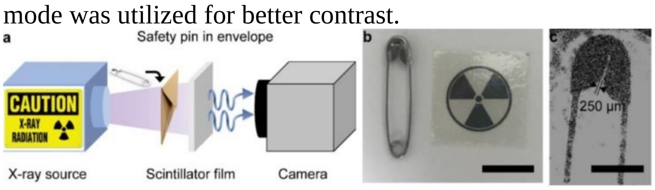

Fig. 3. a) Schematic depiction of the X-ray imaging setup. b) Transparent Li-PEA_2PbBr_4 film on glass substrate next to a safety pin. Scale bar is 1 cm. c) Imaging of the safety pin using the perovskite scintillator film shown in (b). A Cu-Ka source (8.0 keV; 1 mA; 35 keV) was used. Scale bar is 5 mm.

Detection of particles is also a crucial tool for both fundamental research and practical applications. In our work we used Li-$(PEA)_2PbBr_4$ crystals for alpha-particle (α) and neutron (n) detection. Fig. 4a displays the result of alpha particle pulse height characterization of Li-doped crystal using ^{241}Am (5,49 keV) and ^{244}Cm (5,81 keV) alpha particle sources. We can easily distinguish the two photo-peaks although they are relatively broad. The photo-peaks indicate the potential thermal neutron detection on the alpha particle as a product from the ^{6}Li (n, α) reaction. Fig. 3b shows the first sign for pulse shape discrimination (PSD) with our Li-$(PEA)_2PbBr_4$ crystals (Fig. 4b inset). The alpha particle signal is distinctly separated from gamma-ray signal, with some small signal overlap. We also can discriminate the high energy radiations between thermal neutrons and gamma-rays as shown in Fig. 4c. An even stronger signal is expected if pure ^{6}Li (which is only 7.6 % of the total naturally occurring Li-isotopes) is to be used as dopant.

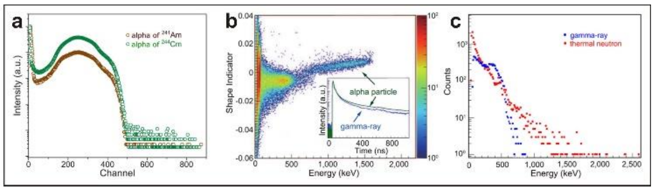

Fig. 4. Alpha particle detection, pulse shape discrimination and thermal neutron. a) Alpha particle pulse height spectra, b) pulse shape discrimination (PSD) matrix with the shape indicator on y-axis and the measured energy (electron equivalent) on x-axis and c) pulse height spectra measured of thermal neutron (red dots) and ^{137}Cs sources (blue dots) of 1:1 Li-$(PEA)_2PbBr_4$ crystal. The inset with the green and the blue curves shows the normalized average waveforms from both gamma-ray and alpha particle radiation of ^{137}Cs and ^{241}Am sources, respectively.

3. Conclusions

In conclusion, both perovskite QDs and crystals have great potentials for radiation imaging applications since both have strong emission responses from high-energy excitations. However, due to their good energy resolution with spectroscopy, 2D perovskite crystals have broader applications involving gamma-ray, alpha particle, and thermal neutron such as positron emission tomography, landmine detection, and oil lodging.

Acknowledgements

The authors acknowledge financial supports from the Singapore Ministry of Education (MOE2019-T1-002-087) and Thales-CINTRA Funding.

References

1. Birowosuto, M.D., et al., *X-ray Scintillation in Lead Halide Perovskite Crystals.* Sci. Rep., 2016. **6**: p. 37254.
2. Chen, W., et al., *X-ray radioluminescence effect of all-inorganic halide perovskite CsPbBr3 quantum dots.* Journal of Radioanalytical and Nuclear Chemistry, 2017. **314**(3): p. 2327-2337.
3. Maddalena, F., et al., *Inorganic, Organic, and Perovskite Halides with Nanotechnology for High–Light Yield X- and γ-ray Scintillators.* Crystals, 2019. **9**(2): p. 88.
4. Tsai, H., et al., *Stable Light-Emitting Diodes Using Phase-Pure Ruddlesden–Popper Layered Perovskites.* Advanced Materials, 2018. **30**(6): p. 1704217.
5. Mao, L., et al., *White-Light Emission and Structural Distortion in New Corrugated Two-Dimensional Lead Bromide Perovskites.* Journal of the American Chemical Society, 2017. **139**(14): p. 5210-5215.
6. Chen, Q., et al., *All-inorganic perovskite nanocrystal scintillators.* Nature, 2018. **561**(7721): p. 88-93.
7. Xie, A., et al., *Lithium-doped two-dimensional perovskite scintillator for wide-range radiation detection.* Comms. Mater., 2020. **1**(1): p. 37.
8. Xie, A., et al., *Library of Two-Dimensional Hybrid Lead Halide Perovskite Scintillator Crystals.* Chem. Mater., 2020. **32**(19): p. 8530-8539.